Materials Research. 2013; 16(1): 158-163
DOI: 10.1590/S1516-14392012005000162

Nanostructured MgH_2 Obtained by Cold Rolling Combined with Short-time High-energy Ball Milling

***Ricardo Floriano*[a]*, *Daniel Rodrigo Leiva*[b], *Stefano Deledda*[c], *Bjørn Christian Hauback*[c], *Walter José Botta*[d]**

[a]*Programa de Pós-graduação em Ciência e Engenharia de Materiais, Universidade Federal de São Carlos – UFSCar, Rod. Washington Luiz, Km 235, CEP 13565-905, São Carlos, SP, Brasil*
[b]*Faculdade de Ciências Aplicadas, Universidade Estadual de Campinas – UNICAMP, Rua Pedro Zaccaria, 1300, CEP 13484-350, Limeira, SP, Brasil*
[c]*Physics Department, Institute for Energy Technology, PO Box 40, N-2027 Kjeller, Norway*
[d]*Departamento de Engenharia de Materiais, Universidade Federal de São Carlos – UFSCar, Rod. Washington Luiz, Km 235, CEP 13565-905, São Carlos, SP, Brasil*

Received: June 7, 2012; Revised: August 23, 2012

MgH_2 was processed by short time high-energy ball milling (BM) and cold rolling (CR). A new alternative processing route (CR + BM) using the combination of CR followed by short time BM step was also applied. The effects on the final morphology, crystalline structure and H-sorption properties were evaluated. The CR + BM processing (compared to BM and CR process) resulted in an inhomogeneous particle size distribution and the biggest crystallite size of MgH_2, showing that there is a clear dependence between the size/shape of the particles which compose the starting material and the efficiency of crystallite size reduction during the BM process. On the other hand, we observed that a short BM step improved the kinetic properties of the cold rolled material. It shows that the particle size reduction of MgH_2 obtained by CR combined with the increase in specific surface area attained by short BM step could be key factors to allow the use of the CR + BM route.

Keywords: *magnesium hydride, cold rolling, high-energy ball milling, nanostructures*

1. Introduction

In spite of its high desorption temperature and slow kinetics, MgH_2 is still considered a good candidate for hydrogen storage applications due its high hydrogen storage reversible capacity, 7.6 wt. (%), and low cost[1].

Many studies[2-5] have shown that processing of MgH_2 by high-energy ball milling techniques can result in nanocrystalline structures with relatively low desorption temperatures and good H-sorption kinetics. These results are easily enhanced with elemental or compound additives, such as, transition metals and their fluorides and oxides.

However, the high consumption of energy, the high cost and longer processing times involved in ball milling techniques are still drawbacks from the upscale point of view. Furthermore, the poor air-resistance to oxidation associated with the fine powder product produced requires a complex and expensive handling process.

In this scenario, severe plastic deformation (SPD) techniques such as *High Pressure Torsion* (HPT), *Equal Channel Angular Pressing* (ECAP), *Cold forging* (CF) and *Cold rolling* (CR) have recently been explored to process/synthesize metal hydrides resulting in materials with hydrogen storage properties as good as ball milling techniques[6-9].

In addition to the refined nanocrystalline structure and presence of selective catalyst elements, the remarkable improvements on hydrogen storage properties have also been related to the presence of metastable phases (such as γ-MgH_2), introduction of a high density of defects and modification of the texture in the processed materials.

More recently it has been shown that cold rolling could be successfully performed on the fully hydrided MgH_2 resulting in a nanocrystalline structure and reduction of crystallite size similar to the one obtained by ball milling[10-12].

Other remarkable aspects of cold rolling processing of MgH_2 are the important reduction in processing time and energy and the possibility of handling the material under air atmosphere during all processing without negative effect on the hydrogen storage capacity or the kinetic properties.

In the present study, MgH_2 has been processed by a new alternative processing route involving cold rolling and short time high energy ball milling. The crystal structure, morphology and hydrogen storage properties from the MgH_2 samples have been investigated.

*e-mail: ricardo_fisica@hotmail.com

2. Experimental

2.1. *Samples preparation*

Commercial MgH_2 (Alfa Aesar, 98%) powders were processed by cold rolling (CR), ball milling (BM), and cold rolling followed by a short-time ball milling step (CR + BM). For the CR sample, the MgH_2 powder was confined between two stainless plates and processed in a commercial powerful duo-reversible FENN rolling mill, applying up to five passes with 75% of reduction in each pass. The number of passes was limited to five due to close distance between the rolls. The CR process was done in air. In the case of the BM sample, the MgH_2 powder was inserted in a stainless crucible with stainless steel balls in a glove box under argon atmosphere. The ball milling experiment was carried out in a SPEX mill for 20 minutes with a ball-to-powder weight ratio of 40:1. The balls diameter of 10 mm and material mass of 1 g were used. The CR + BM sample was prepared using the same conditions applied to the other samples separately, namely, cold rolled five times followed by short ball milling step for 20 minutes.

2.2. *Characterization techniques*

Microstructural characterization of the samples was carried out by X-ray diffraction (XRD) and scanning electron microscopy (SEM). XRD patterns were recorded with a Siemens diffractometer (Model D5005) equipped with a C-monochromator using monochromatic Cu Kα radiation (40 kV and 40 mA). The XRD data was also used to calculate the mean crystallite size through Scherrer analysis[13]. For that, the contribution of the instrumental broadening was deconvoluted using a known pattern (Corundum). SEM images were obtained in a Philips XL-30 TMP Microscope.

The hydrogen desorption behavior of the samples was investigated by differential scanning calorimetry (DSC) coupled with a quadrupole mass spectrometry (QMS), performed in a NETZSCH assembly (STA 449C and QMS403C, respectively). Samples with mass around 10 mg were used. The measurements were performed with a heating rate of 10 K/min.

The H-sorption properties after the first desorption were evaluated with a volumetric PCT apparatus built in-house at Institute for Energy Technology (IFE), using samples with mass of around 140 mg. Absorption and desorption curves were recorded at 623 K, with pressures of 2 MPa and 0.05 MPa, respectively. The procedures to measure the absorption/desorption kinetic curves and to calculate the hydrogen capacity using a volumetric apparatus are found in Léon[17].

3. Results and Discussion

3.1. *Scanning electron microscopy*

Figure 1 presents the SEM micrographs of as-received MgH_2, CR, BM and CR + BM samples. The as-received sample has worm-like shaped particles with a width of about 10-20 μm and length of the order 200 μm. In the micrograph for the CR sample, the MgH_2 powders are transformed into very well consolidated small plates, showing that cold rolling is a good method for powder agglomeration. This was shown also by Lang and Huot[11] using a different (vertical) rolling mill. For the BM and CR + BM samples, the SEM micrographs show a random size distribution of particles with average size around 1-20 μm, hence smaller than the particles in the as-received sample. Furthermore, the size distribution seems to be coarser for the CR + BM sample than for the BM sample. This indicates that short-time BM applied after CR was not enough to homogeneously break all small plates consolidated from the cold rolling, resulting in an irregular particle size distribution. As these consolidated plates coming from the cold rolling process are much harder than the as-received material, different morphological products are obtained which is strongly related to the hardening level of the starting material.

During the BM process, the big MgH_2 particles are constantly broken into smaller particles as shown in Figure 1.

3.2. *Crystalline structure*

The XRD pattern of as-received MgH_2 (Figure 2) shows the predominant β-MgH_2 and remaining Mg. Furthermore, a small contamination with $Mg(OH)_2$ is observed, appearing also in the processed samples (Figure 3). Figure 3 presents XRD patterns of the CR, BM and CR + BM samples. The Bragg peaks of these samples are much broader than for the as-received sample (Figure 2). A closer inspection shows that the Bragg peaks of the BM sample are even broader than the other samples. The peak broadening is a clear indication of the presence of a nanocrystalline microstructure, resulting from the formation of defects and the crystallite size reduction processes.

Values for the average crystallite size were estimated using the Scherrer formula and are given in the Table 1. The angle 2θ used to calculate the crystallite size is around 36°. The processed samples (Figure 3) show a significant reduction in the crystallite size compared to the as-received sample (>100 nm). The average crystallite size for the BM sample is 11 nm while for the CR sample is 22 nm. The value of the average crystallite size for the BM sample is much smaller than the value found in Imamura[18] (~23 nm). While in Lang and Huot[11], the value found for the average crystallite size (~13 nm) can be considered equivalent to our value. Although the slight differences in the BM conditions, our results indicate that, under the conditions used in this work, BM is more effective to reduce the crystallite size than CR.

However, the nature of starting material and, most of all, the initial crystallite size of the MgH_2 particles can exert an important role in the efficiency of the crystallite size reduction during ball milling. As observed in the Table 1, the CR + BM sample has the largest crystallite size around 29 nm even after being submitted to both processes (cold rolling followed by ball milling). An acceptable explanation for this result is the occurrence of recrystallization phenomenon during ball milling step. The stored energy due to the high number of crystalline defects in the deformed state after cold rolling and the combination of the increase in temperature during ball milling and attempt to create new defects act as driving force for the nucleation and growth processes of stress-free grains[14].

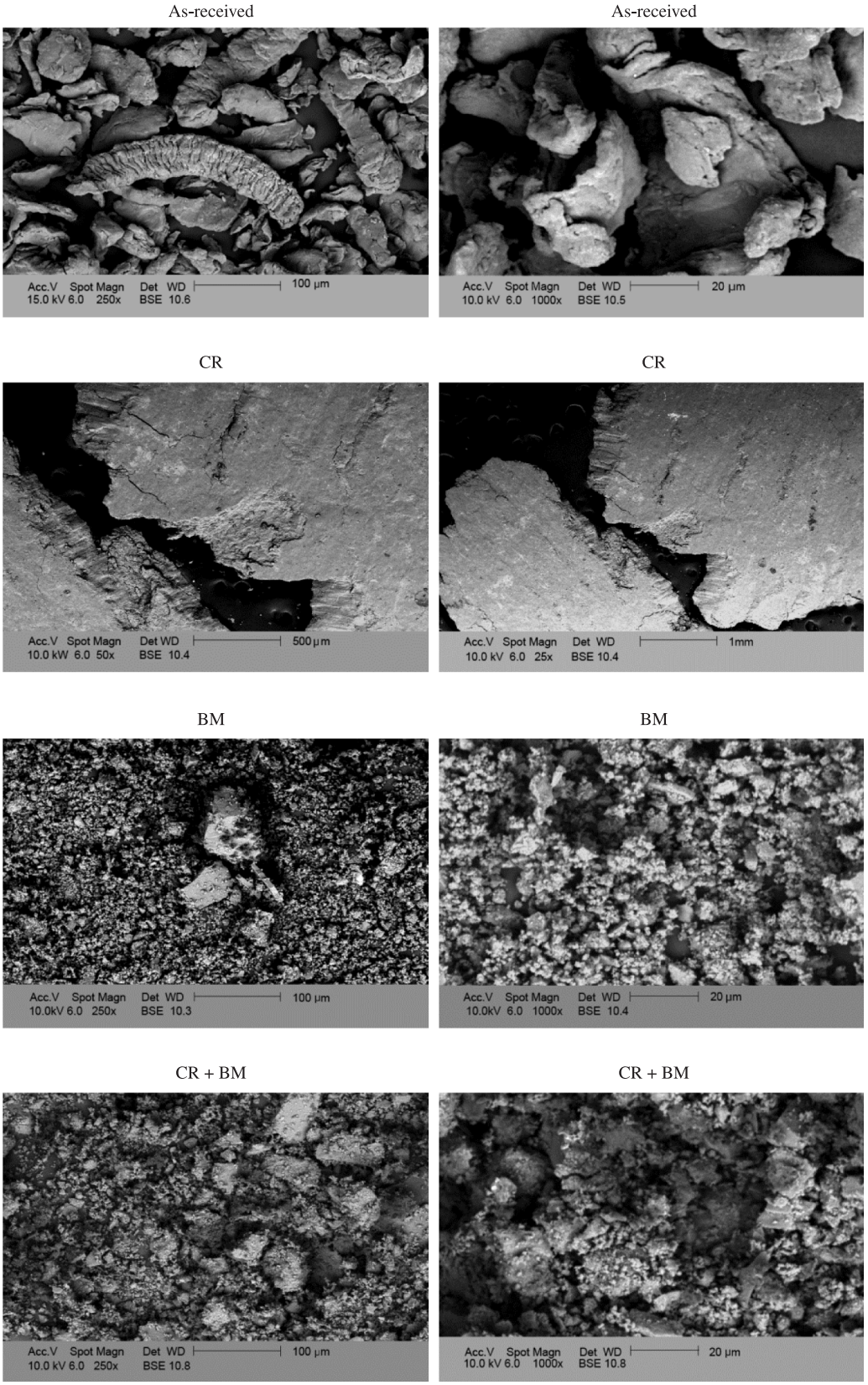

Figure 1. SEM micrographs for commercial MgH_2 (As received), cold rolled five times (CR), ball milled for 20 minutes (BM) and cold rolled + ball milled (CR + BM).

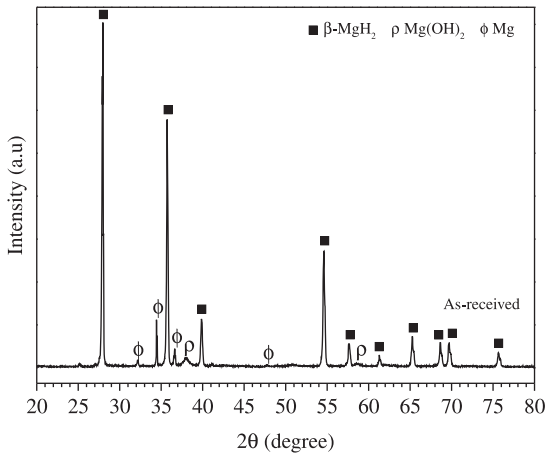

Figure 2. X-ray diffraction pattern for commercial as-received MgH_2.

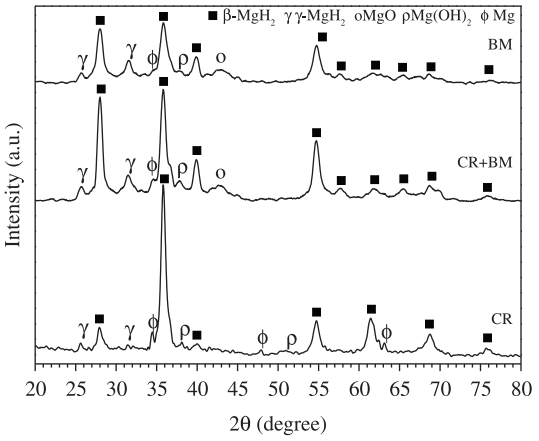

Figure 3. X-ray diffraction patterns for MgH_2: Cold rolled five times (CR, bottom), ball milled for 20 minutes (BM, top) and cold rolled + ball milled (CR + BM, middle).

Table 1. Values for the average crystallite size.

Samples	Crystallite size (nm)
As-received	>100
CR	22(4)
BM	11(5)
CR + BM	29(3)

A significant preferred orientation along the (011) direction is observed only in the XRD pattern for the CR sample ($2\theta \approx 36°$). We have previously reported this effect[8].

The XRD patterns of all processed samples show that the β-MgH_2 phase has partially been converted to the high pressure γ-MgH_2 phase. The formation of γ-MgH_2 during CR and BM of MgH_2 has previously been discussed by Lang and Huot[11]. They pointed out that, compared to the BM process performed in 30 minutes, its formation after five passes of CR process requires shorter activation times and less energy.

MgO was identified in the XRD patterns after ball milling (that is, for both BM and CR+BM samples), whereas it was not observed in the CR sample. The formation of MgO is a very common and is related with the large specific surface area available in the samples when processed by ball milling[2].

3.3. *DSC measurements*

Figure 4 shows DSC curves for CR, BM and CR + BM samples compared with the as-received powder. Table 2 presents data from the DSC (Onset temperature; T_{onset}) and the qualitative QMS analysis. The peak temperature is indicated in each curve.

The DSC curves for all processed samples show a significant decrease in the desorption temperature compared with the as-received powder. For the CR sample, the reduction in desorption temperature is observed despite the large reduction in the specific surface area caused by the cold rolling process. This was attributed to the grain (sub-grain) refinement produced by the cold rolling process[8].

It should be noted that the BM and CR + BM samples show double DSC peaks while the CR sample presents only one asymmetric peak. The double peak is more distinct for the CR + BM sample than for the BM sample, but the peak temperature observed in the low-temperature DSC peak are similar in both samples. The existence of double peak in the DSC curves can be associated with the total decomposition of the high pressure γ-MgH_2 phase (identified in the XRD patterns) and the simultaneous partial decomposition of β-MgH_2 in the low-temperature DSC peak, whereas the high-temperature DSC peak corresponds to β-MgH_2 decomposition to Mg[15]. At the same time, the presence of the double DSC peak can also be attributed to the inhomogeneous distribution in the particle size, as seen in the micrographs of the samples[16], especially for the CR + BM sample. The QMS analysis indicated that all endothermic events detected by DSC are related to hydrogen desorption from MgH_2.

3.4. *Hydrogen sorption properties*

The hydrogen absorption and desorption kinetic curves for the BM, CR and CR + BM samples are shown in Figures 5 and 6, respectively. The as-received sample displayed a very slow absorption and desorption kinetics during the time interval that was studied and therefore these curves are not shown here. Some general features can be observed in Figures 5 and 6: all samples show very good H-sorption properties with hydrogen storage capacities around 5.3 wt. (%) and sorption times in the range of minutes. However, some differences in the kinetic behavior and shape between the curves are observed.

The absorption and desorption kinetics started faster for the samples in the following sequence: BM, CR + BM and CR. At absorption, the storage capacity of the BM sample is slightly higher than for the CR + BM and CR samples, the latter samples showing the same storage capacity.

For the CR + BM sample, the kinetics during the first 4 minutes of desorption is slightly faster than the BM sample as can be seen in the inset graph of the Figure 6. In addition, the kinetic of the CR+BM sample is better than for the CR sample, which means in a faster kinetic than CR sample. This shows the importance of short ball milling after the cold rolling process in order to produce more surface area which is one of the key factor for good kinetics behavior.

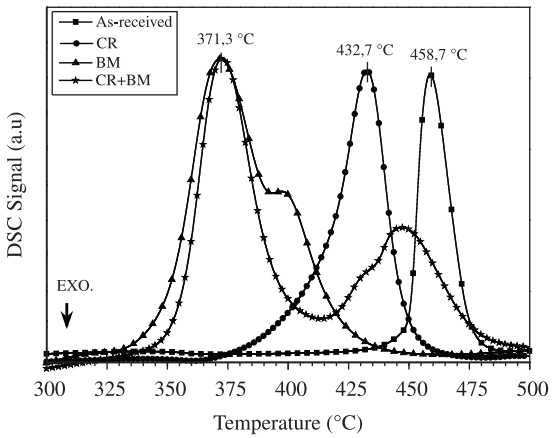

Figure 4. DSC curves for MgH_2: As received, cold rolled five times (CR), ball milled for 20 minutes (BM) and cold rolled + ball milled (CR + BM). The values for the peak temperatures are included in the figure.

Table 2. Onset temperature (T_{onset}) and QMS analysis from the DSC peaks.

Samples	T_{onset} (°C)	QMS
As-received	449,5	H_2
CR	409,0	H_2
BM	347,8	H_2
CR + BM	350,3	H_2

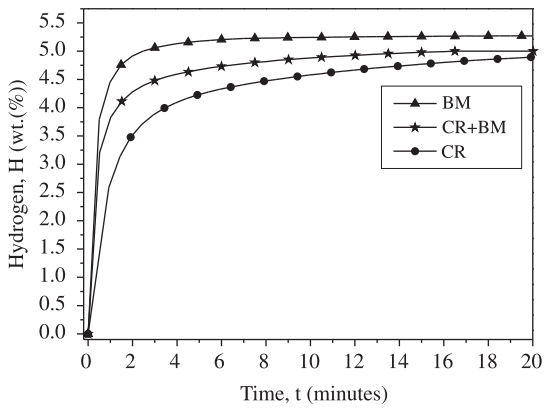

Figure 5. Absorption kinetics at 623 K and under 2 MPa hydrogen pressure for MgH_2: cold rolled five times (CR), ball milled for 20 minutes (BM) and cold rolled+ball milled (CR + BM).

The kinetic behavior showed by the CR sample is in agreement with our previous papers[8,10], and could be explained considering two possible reasons: a) the nanoscale grain (sub-grain) refinement; b) the better heat transfer due to the consolidation of particles in small plates.

In general, these results indicate that there is an important compromise between the particle size distribution, surface area and the kinetic behavior. For this reason, the processing route chosen should take into account not only the optimization of factors such as processing time, cost

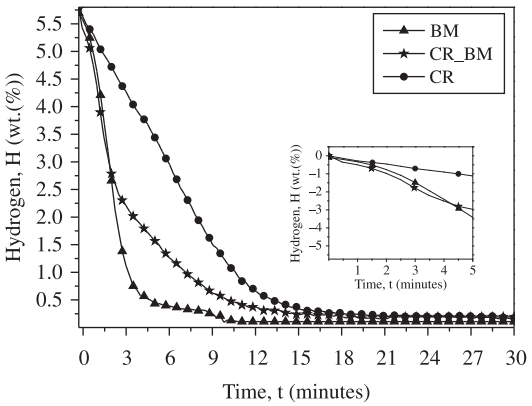

Figure 6. Desorption kinetics at 623 K and under 0,05 MPa hydrogen pressure for MgH_2: cold rolled five times (CR), ball milled for 20 minutes (BM) and cold rolled+ball milled (CR + BM).

and scalable application, but also, the ability to produce materials with a very refined structure with a homogenous particle size distribution.

4. Conclusions

A significant decrease of desorption temperature range was observed in the DSC analysis of all processed samples compared to as-received sample. The BM and CR + BM samples presented double DSC peak both with lower temperature compared to the CR sample.

We observed that short-time BM improves the kinetic properties of the cold rolled material. At the same time, the efficiency of particle size reduction during BM is strongly dependent of the size and shape of the particles which compose the starting material. This result could be noticed when the short BM step was applied in a MgH_2 sample already processed by CR whose initial product submitted to the BM step is a deformed material with size and shape of particles different of a MgH_2 sample only processed by BM, that in this case, the initial state of the sample is a homogenous powder. Nanocrystalline γ-MgH_2 was found in all MgH_2 processed samples.

Thus, these results indicate that a combined route for SPD processing, which includes a short ball milling step, can be a key factor for achieving better kinetic properties of cold rolled sample.

We also believe that the reduction of processing time achieved by the combination of cold rolling and an additional short milling step can be interesting processing routes for producing materials with enhanced hydrogen properties compared to materials processed separately by cold rolling or ball milling.

Acknowledgements

The authors wish to thank FAPESP by the financial support. Floriano R. also would like to thanks CNPq for a *PhD* scholarship.

References

1. Fu Y, Kulenovic R and Mertz R. The cycle stability of Mg-based nanostructured materials. *Journal of Alloys and Compounds*. 2008; 464:374-376. http://dx.doi.org/10.1016%2Fj.jallcom.2007.09.129
2. Hanada N, Hirotoshi E, Ichikawa T, Akiba E and Fujii H. SEM and TEM characterization of magnesium hydride catalyzed with Ni nano-particle or Nb_2O_5. *Journal of Alloys and Compounds*. 2008; 450:395-399. http://dx.doi.org/10.1016%2Fj.jallcom.2006.10.128
3. Liang G, Huot J, Boily S, Van Neste A and Schulz R. Catalytic effect of transition metals on hydrogen sorption in nanocrystalline ball milled $MgH_2 - T_m$ (T_m = Ti, V, Mn, Fe and Ni) systems. *Journal of Alloys and Compounds*. 1999; 292:247-259. http://dx.doi.org/10.1016%2FS0925-8388%2899%2900442-9
4. Barkhordarian G, Klassen T and Bormann R. Fast hydrogen sorption kinetics of nanocrystalline Mg using Nb_2O_5 as catalyst. *Scripta Materialia*. 2003; 49:213-217. http://dx.doi.org/10.1016%2FS1359-6462%2803%2900259-8
5. Yavari AR, LeMoulec A, De Castro FR, Deledda S, Friedrichs O, Botta WJ et al. Improvement in H-sorption kinetics of MgH_2 powders by using Fe nanoparticles generated by reactive FeF_3 addition. *Scripta Materialia*. 2005; 52:719-724. http://dx.doi.org/10.1016%2Fj.scriptamat.2004.12.020
6. Leiva DR, Jorge AM, Ishikawa TT, Huot J, Fruchart D, Miraglia S et al. Nanoscale grain refinement and H-sorption properties of MgH_2 processed by high-pressure torsion and other mechanical routes. *Advanced Engineering Materials*. 2010; 12:786-792. http://dx.doi.org/10.1002%2Fadem.201000030
7. Skripnyuk V, Rabkin E, Estrin Y and Lapovok R. The effect of ball milling and equal channel angular pressing on hydrogen absorption/desorption properties of Mg–4.95 wt% Zn-0.71 wt% Zr (ZK60) alloy. *Acta Materialia*. 2004; 52:405-414. http://dx.doi.org/10.1016%2Fj.actamat.2003.09.025
8. Leiva DR, Floriano R, Huot J, Jorge AM, Bolfarini C, Kiminami CS et al. Nanostructured MgH_2 prepared by cold rolling and cold forging. *Journal of Alloys and Compounds*. 2011; 509S:444-448. http://dx.doi.org/10.1016%2Fj.jallcom.2011.01.097
9. Huot J. Nanocrystalline metal hydrides obtained by severe plastic deformations. *Metals*. 2012; 2:22-40. http://dx.doi.org/10.3390%2Fmet2010022
10. Leiva DR, Huot J, Ishikawa TT, Bolfarini C, Kiminami CS, Jorge AM et al. Hydrogen Activation Behavior of Commercial Magnesium Processed by Different Severe Plastic Deformation Routes. *Materials Science Forum*. 2011; 667-669:1047-1051. http://dx.doi.org/10.4028%2Fwww.scientific.net%2FMSF.667-669.1047
11. Lang J and Huot J. A new approach to the processing of metal hydrides. *Journal of alloys and compounds*. 2011; 509:L18-L22. http://dx.doi.org/10.1016%2Fj.jallcom.2010.09.173
12. Vincent SD, Lang J and Huot J. Addition of catalysts to magnesium hydride by means of cold rolling. *Journal of Alloys and Compounds*. 2012; 512:290-295. http://dx.doi.org/10.1016%2Fj.jallcom.2011.09.084
13. Lu L and Lai MO. *Mechanical Alloying*. Boston: Kluwer; 1998. http://dx.doi.org/10.1016%2FS0921-5093%2898%2900676-5
14. Reed-Hill RE. *Physical Metallurgy and Principles*. 2nd ed. D.Van Nostrand Company; 1973.
15. Gennari FC, Castro FJ and Urretavizcaya G. Hydrogen desorption behavior from magnesium hydrides synthesized by reactive mechanical alloying. *Journal of alloys and compounds*. 2001; 321:46-53. http://dx.doi.org/10.1016%2FS0925-8388%2800%2901460-2
16. Varin RA, Czujko T, Chiu C and Wronski Z. J. Particle size effects on the desorption properties of nanostructured magnesium *dihydride* (MgH_2) synthesized by controlled reactive mechanical milling (CRMM). *Journal of Alloys and Compounds*. 2006; 424:356-364. http://dx.doi.org/10.1016%2Fj.jallcom.2005.12.087
17. Léon A, editor. *Hydrogen Technology*. Berlin: Springer-Verlag; 2008. chapt. 16: Kinetics and Thermodynamics.
18. Imamura H, Masanari K, Kusuhara M, Katsumoto H, Sumi T and Sakata Y. High hydrogen storage capacity of nanosized magnesium synthesized by high energy ball-milling. *Journal of Alloys and Compounds*. 2005; 386:211-216. http://dx.doi.org/10.1016%2Fj.jallcom.2004.04.145